

## Sensitivity analysis for seismic source characteristics to probabilistic seismic hazard assessment in central Apennines (Abruzzo area)

L. PERUZZA<sup>(1)</sup> and B. PACE<sup>(2)</sup>

<sup>(1)</sup>*OGS Istituto Nazionale di Oceanografia e di Geofisica Sperimentale, Trieste, Italy*

<sup>(2)</sup>*GeoSisLab, Dipartimento di Scienze della Terra, Univ. D'Annunzio, Chieti, Italy*

(Received April 10, 2002; accepted June 30, 2002)

**Abstract** - This paper presents the results of an analysis showing the effect of different assumptions of magnitude recurrence and time dependence on probabilistic seismic hazard assessment for the Abruzzo area. The focus is on alternative peak ground acceleration maps for the whole area and disaggregation analysis for three main towns (L'Aquila, Sulmona and Avezzano). The source model of regional relevance has been defined by: 1) definition of primary source faults on a geological-structural basis; 2) drawing of seismogenic boxes with computation of parameters such as maximum magnitude and relative mean recurrence, based on geometrical and kinematic elements; 3) association of a proper seismicity model consistent with the historical information available. The final seismic hazard assessment incorporates a renewal-time, characteristic-magnitude model for the larger earthquakes, with a conventional exponential-time, exponential-magnitude model for the smaller events, depending on the knowledge of the sources. The hybrid method used here seems to be adequate in modelling earthquake occurrences in fault-specific cases; using the surface projection of 3D sources, we approximate the computations to obtain results suitable for engineering applications. The hypotheses for seismicity models are wide ranging, and are all in some way realistic, because they are based on different earthquake catalogue interpretations, rare paleoseismological data, no geodynamic measurement constraints (at least till now). But, the more we are willing to abandon simplistic assumptions, such as the Gutenberg-Richter law or the characteristic-earthquake model, the more accurately we have to model the implications of all the available information. The disaggregation analysis, in particular, shows how valuable the use of the long history of seismic shaking of some localities is, in assessing the need to model a time-dependent recurrence in the analyses.

---

Corresponding author: L. Peruzza, Ist. Naz. di Oceanografia e di Geofisica Sperimentale, Borgo Grotta Gigante 42c, 34010 Sgonico (Trieste), Italy; phone +39 0402140244; fax +39 040327307; e-mail: lperuzza@ogs.trieste.it

## 1. Introduction

Recent earthquake sequences in central Italy again raise the problem of recognizing seismogenic faulting and seismic rate estimation for those that have been silent during historical times (Amato et al., 1998; Barba and Basili, 2000; Tondi, 2000; Valensise and Pantosti, 2001a). This is a topic of particular importance in seismic hazard assessment, as nowadays, in Italy, it is quite accepted that the national earthquake catalogues may not be adequate to represent all the sources of medium-to-strong events. In addition, experiments to introduce time dependence into the process make it clear that this may be a first-order element driving the results, although most of the assumptions and ingredients are very difficult to define (Barchi et al., 2000; Peruzza, 1999a). Although this matter appears limited to a research problem, with no apparent practical application, sensitivity analyses will serve to suggest the most critical parameters to be defined, and the most reliable way of filling the gaps in the knowledge. The aim of this paper, together with other analyses focused in the northern sector of the central Apennines (Pace et al., 2002a), is to explore how to quantify the seismicity from a source-model based mainly on structural and geological data, and the consequences in terms of predicted probabilistic hazard.

## 2. Source model

The geometry of the sources and the seismicity model associated with them drive the results of probabilistic seismic hazard analyses. These are described below.

### 2.1. Seismogenic zonation

Over the past years, many authors investigated the problem of identifying active faulting in the central Apennines, and of assessing their seismogenic role (e.g., Barchi et al., 2000; Galadini and Galli, 2000; Valensise and Pantosti, 2001a, 2001b). In particular, recent papers (Lavecchia et al., 2002; Pace et al., 2002a; Boncio et al., 2002) have identified and proposed some “seismogenic master faults”, by integrating surface geology and subsurface structural data, with historical and good-quality instrumental seismological data. The term “seismogenic master fault” defines a fault structure of regional importance, in some cases segmented at the surface in closely-spaced structures of minor hierarchical order, but substantially continuous for several kilometers at depth. The criteria for defining master faults are one or more of the following: 1) evidence of activity in Holocene-late Pleistocene times; 2) paleoseismological evidence; 3) activation during instrumental seismic sequences and/or association with historical earthquakes; 4) continuity and kinematic compatibility with adjacent faults satisfying the previous requirements.

The seismogenic master faults recognized in the Abruzzo area have been mapped in Fig. 1a; the identification number derives from a wider set of seismogenic sources of the central Apennines discussed elsewhere (Pace, 2001). The most doubtful structures, in terms of possi-

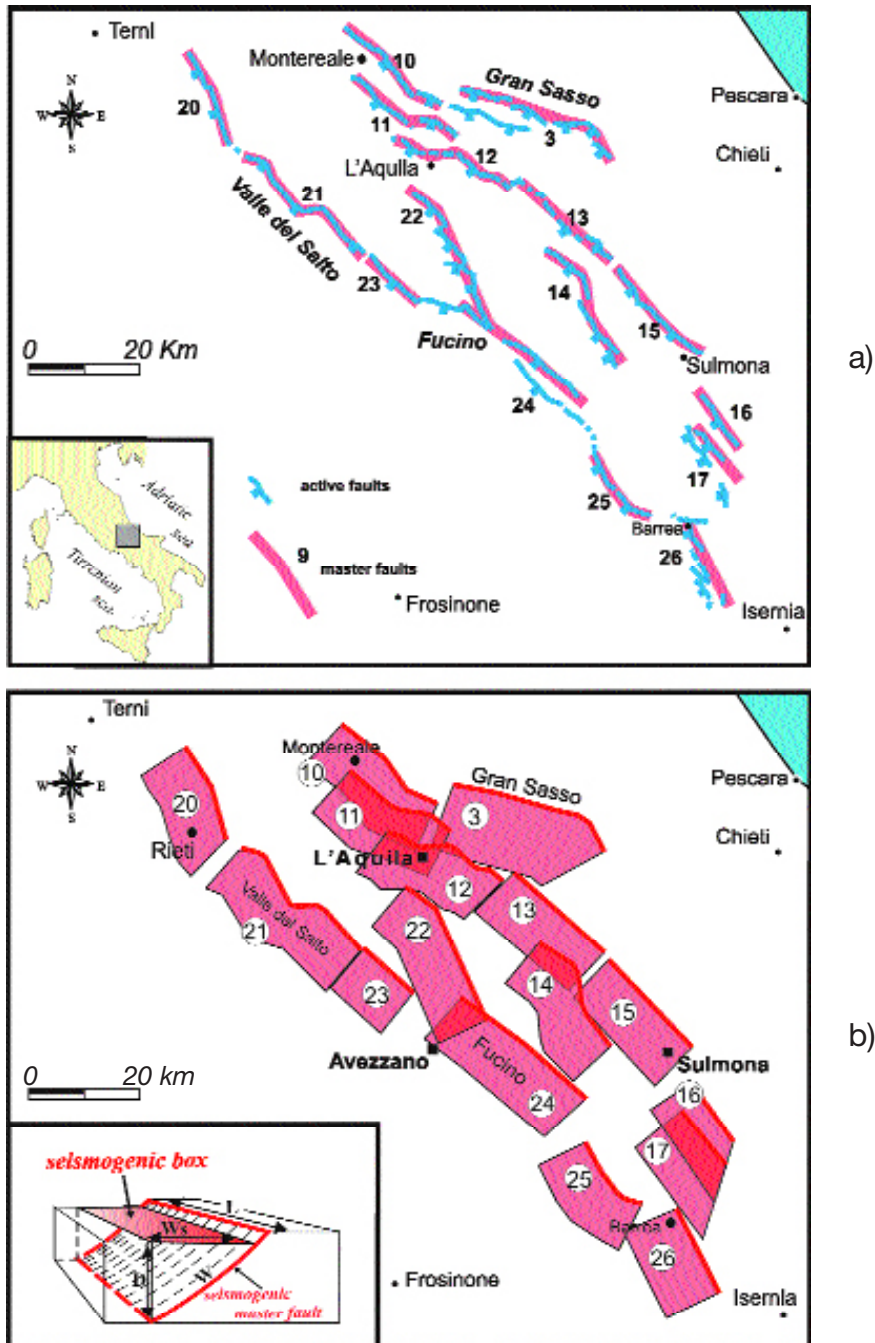


**Fig. 1** - Seismogenic source model for the study region. a) Map of the Abruzzo Quaternary normal faults of seismogenic significance; black numbers refer to the seismogenic master fault (thick red lines) mentioned in the text: 3: Gran Sasso; 10: Montereale-Monte San Franco; 11: Pizzoli-Monte Stabiate; 12: Aquilano; 13: Aterno; 14: Conca Subequana; 15: Sulmona; 16: Pizzalto; 17: Aremogna-Cinque Miglia; 20: Rieti; 21: Valle del Salto; 22: Campo Felice-Ovindoli; 23: MonteVelino; 24: Fucino; 25: Montagna Grande-Val di Sangro; 26: Barrea. b) Map of the Abruzzo seismogenic boxes; thick red lines are the surface trace of seismogenic master faults of Fig. 1a. The 3D scheme of a seismogenic box is given in the lower left angle:  $W_s$  = surface box width;  $L$  = along-strike length of the seismogenic fault;  $W$  = down-dip length of the seismogenic fault,  $D$  = thickness of the local seismic layer (i.e. maximum depth-extent of the seismogenic fault plane).

**Table 1** - Geometric parameters of the seismogenic boxes in the Abruzzo area: *L* = along master fault strike length; *D* = thickness of the local seismogenic layer; *Ws* = width of the projection in surface of the fault surface; *W* = width along master fault dip length; *RA* = maximum rupture area. *SR* is the slip rate attributed to the sources.

BOX	<i>L</i> (km)	<i>D</i> (km)	<i>Ws</i> (km)	<i>W</i> (km)	<i>RA</i> (km <sup>2</sup> )	<i>SR</i> (mm/y)
3) Gran Sasso	32.5	13.5	13.0	17.6	572.7	0.8
10) Montereale-Monte San Franco	23.0	13.5	10.0	17.6	405.3	0.8
11) Pizzoli-Monte Stabiata	23.0	13.0	10.0	17.0	390.3	0.6
12) Aquilano	24.5	13.0	10.0	17.0	415.8	0.6
13) Aterno	22.5	13.0	10.0	17.0	381.8	0.3
14) Conca Subequana	25.0	13.0	10.0	17.0	424.3	0.3
15) Sulmona	22.5	13.0	10.0	17.0	381.8	0.6
16) Pizzalto	16.5	12.0	9.0	17.0	280.0	0.4
17) Aremogna-5Miglia	16.5	13.0	11.5	18.4	303.3	0.4
20) Rieti	19.0	13.0	10.0	17.0	322.4	0.5
21) Valle del Salto	30.0	13.0	10.0	17.0	509.1	0.5
22) Campo Felice-Ovindoli	29.5	13.0	10.0	17.0	500.6	0.8
23) Monte Velino-Magnola	12.5	13.0	10.0	17.0	212.1	0.5
24) Fucino	32.0	13.5	10.0	17.6	563.9	0.6
25) Montagna Grande-Val di Sangro	16.5	13.5	10.0	17.6	290.8	0.6
26) Barrea	17.5	13.5	11.0	17.6	308.4	0.4

ble deep interaction or segmentation criteria are the master faults: 10 Montereale-Monte San Franco, 11 Pizzoli-Monte Stabiata, 12 Aquilano, 13 Aterno, 14 Conca Subequana and 21 Valle del Salto. In particular, these structures present the problem of how overlapped sources can interact and on how to determine the maximum length of the sources without strong evidence of segmentation. On the basis of existing knowledge, the interpretation which identifies these faults seems to be the best supported by data.

**Table 2** - Earthquake association adopted for the boxes; question mark indicates the doubtful cases. The magnitude type is according to CPTI G.d.L. (1999).

BOX	associated earthquakes	
	instrumental	historical
3) Gran Sasso	/	/
10) Montereale-Monte San Franco	/	1703-01 Me = 6.8
11) Pizzoli-Monte Stabiata	/	1703-02 Me = 6.7
12) Aquilano	/	1315 (?) Mm = 6.0; 1791 Mm = 5.1
13) Aterno	/	1461 Me = 6.1; 1762 Me = 5.5
14) Conca Subequana	/	/
15) Sulmona	/	200 A.D. M = ?
16) Pizzalto	/	1315 (?) Mm = 6.0
17) Aremogna-5Miglia	/	1315 (?) Mm = 6.0 801 A.D. M = ?
20) Rieti	/	1298 Me = 6.2; 1898 Me = 5.3
21) Valle del Salto	/	1349 (?) Me = 7.1
22) Campo Felice-Ovindoli	/	1349 (?) Me = 7.1
23) M.Velino-Magnola	/	1904 Me = 5.5
24) Fucino	/	1915 Me = 7.0
25) Montagna Grande-Val di Sangro	/	/
26) Barrea	1984 Mw = 5.8	/

To give a planar representation of the master faults, useful for probabilistic seismic hazard studies, the authors introduced the concept of “seismogenic box” (Fig. 1b, lower left corner); the shape and dimension of each box strictly reflects the three-dimensional geometry of the related master fault. The box can be considered the polygon where well-constrained epicenters are expected to be located and the map projection of the radiating energy source. The epicenters are expected to occur randomly within the box, and the maximum predictable slipping area for the largest single rupture episode is not expected to exit from the perimeter of the box itself. Table 1 reports the geometric parameters of the seismogenic boxes in the Abruzzo area (Fig. 1b), and the slip-rate values (*SR*) obtained through a critical evaluation of the data available. The maximum rupture area (*RA*) has been calculated from the along-strike length (*L*) and the down-dip length (*W*), that is linked to the average inclination and the maximum depth extent of the seismogenic fault plane (*D*, i.e. thickness of the local seismogenic depth). A set of historical and/or instrumental earthquakes is associated to the boxes (Table 2). In particular, the association of historical earthquakes to the structure is based on the analysis of the distribution of the highest intensity data points (DOM database, Monachesi and Stucchi, 1996) of large earthquakes ( $I_0 > VII$ ,  $M \sim 5.5$ ). Boxes 3 Gran Sasso, 14 Conca Subequana, and 25 Montagna Grande-Val di Sangro are considered to be silent during historical times, but they show paleoseismological evidence of strong pre-historic earthquakes (displacement on late Holocene, Barchi et al., 2000; Galadini and Galli, 2000). An archaeologically inferred earthquake which affected the area around Sulmona town around the middle of the 2nd century A.D. (Galadini and Galli, 2001) could be related to the activity of box 15. The other boxes have one or more associated earthquakes (see Table 2). The January and February 1703 ( $M_e = 6.8$  and  $6.7$ , CPTI G.d.L., 1999) earthquakes most likely activated sources 10 Montereale-Monte San Franco and 11 Pizzoli-Monte Stabiata respectively. The 1315 event ( $M_m = 6.0$ , CPTI G.d.L., 1999) is of uncertain location, and could reasonably be attributed to the boxes 12 Aquilano, 16 Pizzalto or 17 Aremogna-Cinque Miglia. Similarly, the 1349 earthquake ( $M_e = 7.1$ , CPTI G.d.L., 1999) may be attributed either to source 21 Valle del Salto or 22 Campo Felice-Ovindoli. On the basis of both geological and seismological data, the 1915 Avezzano earthquake ( $M_e = 7.0$ , CPTI G.d.L., 1999) is surely associated to the 24 Fucino box. The only significant activity instrumentally monitored in recent decades in the study area is the May 1984 ( $M_w = 5.8$ ) sequence, that ruptured the 26 Barrea source (Pace et al., 2002b).

## 2.2. Calibration of geometrical constraints

A critical aspect in the definition of the earthquake source model is the basis for determining the maximum length of the box. In fact, if the total length of a box is used to constrain the maximum extension of the possible rupture, all the criteria limiting this length have a strong impact in terms of maximum potential magnitude as well as recurrence through slip rate. Often, we do not have strong evidence to limit the length, and a unique interpretation in the segmentation model is not realistic. The specific literature dealing with segmentation criteria, scaling laws, and empirical relationships on coseismic data presents some problems, but none

of the authors suggests a solution to limit fault segments in relation to the thickness of the local seismogenic depth. A regression relationship based on the concept of aspect ratio (see Scholz, 1990 for definitions and terminology) has never been proposed; so we decided to calibrate such a relation, to check the maximum possible rupture length, in a box of well-constrained seismogenic thickness. Examining the dataset used by Bonilla et al. (1984), Wells and Coppersmith (1994), Vakov (1996) and Mai and Beroza (2000), we selected about 260 events worldwide. For these earthquakes we computed the unusual regression relationship correlating the length of the possible maximum rupture (segment of fault that may be simultaneously broken, hereinafter indicated as  $L^\#$ ) to its down-dip width ( $W$ ), one of the best-controlled parameters in our study region. The initial data collection has been modified, to eliminate subduction events, earthquakes belonging to known multiple-rupture processes, duplicates, and the  $L/W$  couples coming from inversion techniques (e.g. the values reported in Mai and Beroza, 2000) and not from observational data. Some records have been changed, according to specific studies (Stein and Barrientos, 1985; Pantosti and Valensise, 1990; Hodgkinson et al., 1996). About 180 events were finally kept, to calibrate a linear relationship, where  $a$  and  $b$  are the unknown coefficients:

$$L^\# = a + b W \quad (1)$$

The regression has been differentiated on the basis of different mechanisms (see Fig. 2, and Table 3). The strike-slip earthquake population (Fig. 2a) is characterized by higher  $L^\#$  values, fixing the  $W$  value; on the contrary, normal earthquakes (Fig. 2b) better approximate the rather natural relationship of  $L$  equal to  $W$  (gray dotted line in the graphs), but in this case the sample used cannot be considered statistically robust. Reverse faults (Fig. 2c) seem to confirm that  $L$  could equal  $W$  up to about 6 km, but that afterwards  $W$  seems to constrain  $L$ ,  $L$  being about 2 to 2.5 times  $W$ . The last regression, used in this paper, is the one obtained considering all the earthquakes with prevalent dip-slip kinematics (“all dip-slip” in Fig. 2d and Table 3).

The plot of aspect ratio versus length (Fig. 2e) clearly shows that the longer the fault is, the lower the aspect ratio is. The histogram of the aspect ratio (Fig. 2f) drops to values lower than 0.3 and the dip-slip events are mostly represented in the range 0.4-1.3. This idea suggests considering with special care boxes having aspect ratios out of this range (i.e.  $L \geq 2.5 W$  and  $L \leq 0.75 W$ ). In central Italy, some antithetic structures of regional relevance (i.e. the Altotiberina Fault, Boncio et al., 2000) are considered the downward limit of the possible extent of west-

**Table 3** - Samples and coefficients of the regression of Eq. (1); values in brackets are the statistical error associated to the unknown parameters,  $R$  the correlation coefficient.

	N° samples	$a$	$b$	$R$
reverse	53	-4.4543 (2.4187)	2.1992 (0.16627)	0.8799
strike	98	-7.096 (1.9731)	2.9807 (0.1860)	0.8531
normal	32	3.0939 (2.0895)	1.2501 (0.1657)	0.8093
all dip	85	-2.3725 (1.834)	1.9354 (0.1324)	0.8486
	TOT. 183			

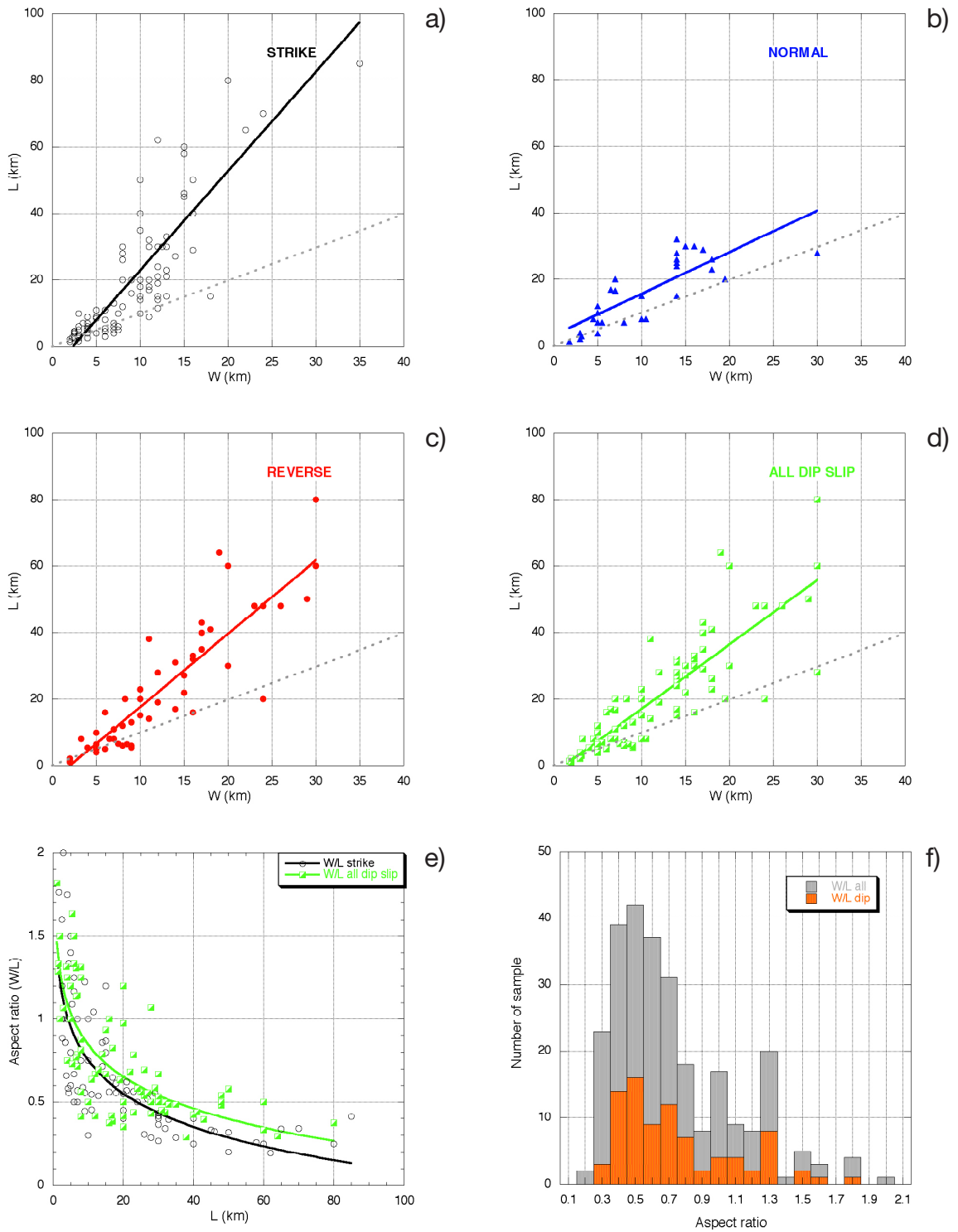


**Fig. 2** - Data used and computed linear relationships of Eq. (1). The regression equations plotted are obtained on the basis of different fault mechanisms (the coefficients and errors are reported in Table 3): a) strike-slip faults; b) normal faults; c) reverse fault; d) normal plus reverse faults; e) aspect ratio versus length; f) aspect ratio histograms for the whole data set (grey) and for the dip-slip mechanisms (orange).

dipping normal faults, controlling the thickness of the local seismogenic depth (5-9 km, Pace, 2001); sometimes, therefore, the boxes drawn exceed the length admitted by the small  $W$  values.

In the Abruzzo area, the  $L^\#$  values (mean values obtained from the regression relationship) have been computed for the boxes that find a general agreement with the length proposed in the segmentation, and confirming, therefore, the accuracy of the adopted seismogenic zonation.

### 2.3. Seismicity rating and models

The first step, in the use of geological data to constrain the input parameters for probabilistic seismic hazard assessment, is the computation of the maximum expected magnitude ( $M_{max}$ ) and the related mean recurrence time ( $T$ ). This has been done on the basis of some geometrical data, such as the maximum length of each box and the maximum rupture area of the source; then, a critical comparison with the observed seismicity may suggest the most adequate model.

Using the parameters of Table 1, we have calculated the related  $M_{max}$  by empirical relationships, calibrated on normal faulting (Wells and Coppersmith, 1994); the  $M_{max}$  has also been calculated from the relationships between fault dimensions and seismic moment. In fact, for a rectangular source with area  $A$ , length  $L$ , width  $W$ , average displacement  $AD$  and shear modulus  $\mu$ , the well-known equation for scalar seismic moment ( $M_0$ ) may be expressed as:

$$M_0 = \mu AD A = \mu AD L W = \mu k L^2 W \quad (2)$$

where  $\mu$  in the crust is  $3 \cdot 10^{10} \text{ Nm}^{-2}$  (Hanks and Kanamori, 1979), and  $k$  is the strain drop, defined as the displacement to length ratio ( $AD/L$ ). In homogeneous seismotectonic regions, constant strain drop is a reasonable assumption (e.g. Scholz, 1990 and references therein). We used the value obtained by Selvaggi (1998), that found a nearly constant value of  $k = 3 \cdot 10^{-5}$  for normal faulting earthquakes in the Apennines by comparing 4 moderate-to-large events (Messina 1908,  $M = 7.0$ ; Avezzano 1915,  $M = 6.7$ ; Irpinia 1980,  $M = 6.9$ ; Umbria-Marche 1997,  $M = 6.0$ ). Magnitude from  $M_0$  has been computed following again Hanks and Kanamori (1979). The maximum expected values for magnitude are plotted in Fig. 3a, where we have also plotted the  $M_{max}$  values obtained by using Eq. (2) on the computed  $L^\#$  values ( $M^\#$ ), in order to check again the consistence of the earthquake sources model. We can note that, using the “seismogenic master faults” proposed by Pace (2001) and Boncio et al. (2002), only four sources reach the most probable  $M_{max}$  constrained by the aspect ratio. The magnitude computed on the geometrical characteristics of the sources varies about 0.2 units, tending to be more dispersed for the smaller structures. The variations are in any case fully comparable with the uncertainties of instrumental data.

Similarly, we have estimated the mean recurrence time ( $T$ ) of the expected maximum magnitude on each box: it has been calculated for the  $M_{max}$  values of Fig. 3a using two different techniques. The first is the ratio of slip per event ( $SE$ ) over the slip rate (values from  $T_1$  to  $T_3$  in Fig. 3b); the first quantity derives from empirical relationships (Wells and Coppersmith,



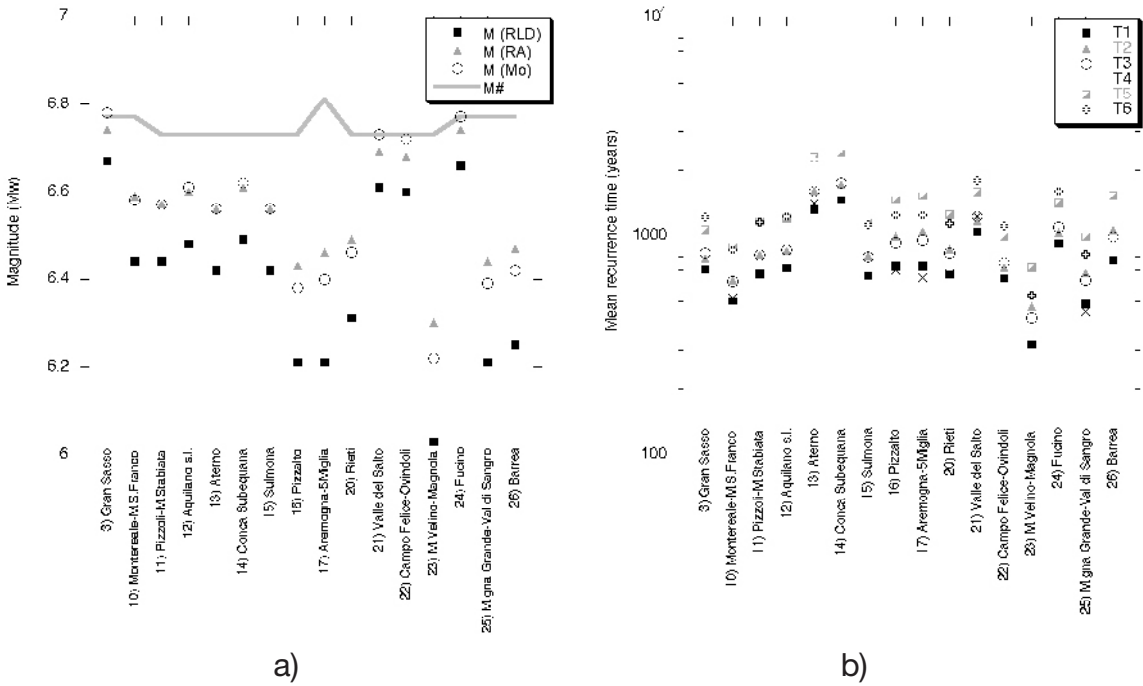


**Fig. 3** - Calibration of maximum earthquakes from geometric/cinematic parameters. a) Maximum expected magnitude ( $M_{max}$ ) values for the Abruzzo seismogenic boxes:  $M(RLD)$  is the moment magnitude from Wells and Coppersmith (1994) relationship on subsurface rupture length;  $M(RA)$  from Wells and Coppersmith (1994) relationship on rupture area;  $M(M_0)$  derives from Eq. (2);  $M^\#$  from  $L^\#$  values (see the text). b) Mean recurrence time associated with the maximum expected earthquake for the Abruzzo seismogenic boxes; the values are calculated from the ratio of slip per event and slip rate ( $T_1$  from  $M(RLD)$ ,  $T_2$  from  $M(RA)$ ,  $T_3$  from  $M(M_0)$ ) and using Eq. (3) ( $T_4$ ,  $T_5$  and  $T_6$  as before).

1994) when not available, and all the information coming from paleoseismological studies have been used (e.g., Blumetti, 1995; Michetti et al., 1996; Pantosti et al., 1996; Galadini and Galli, 2000; D'Addezio et al., 2001; Valensise and Pantosti, 2001b). The second approach ( $T_4$  to  $T_6$  in Fig. 3b) obtains the  $T$  values by using the criteria of the “segment seismic moment conservation”, proposed by Field et al. (1999):

$$1/T = \text{Char\_Rate} = \mu SR L SE/10^{1.5M + 9.05} \tag{3}$$

where Char\_Rate is the annual rate of earthquakes on each source,  $\mu$  is the rigidity modulus and the other parameters are the ones described in Table 1.

Recurrence time estimates vary significantly, more than 30% of the mean values (about 300 years over 1,000, with some worse cases like box 23). Without using Eq. (3), the values are less scattered (about 10-15%), but the slip-ratio method is only apparently more accurate, as nearly all the slip-per-event values are inferred. The variation derives from the magnitude values and from the scaling laws used to obtain the slip-per-event values, as the slip rate is fixed; the actual uncertainties are therefore much higher, and the values obtained here have to be considered as only a first approach to the problem.

Magnitudes from seismic moment ( $M_0$  in Fig. 3a) and their related recurrence times ( $T_6$

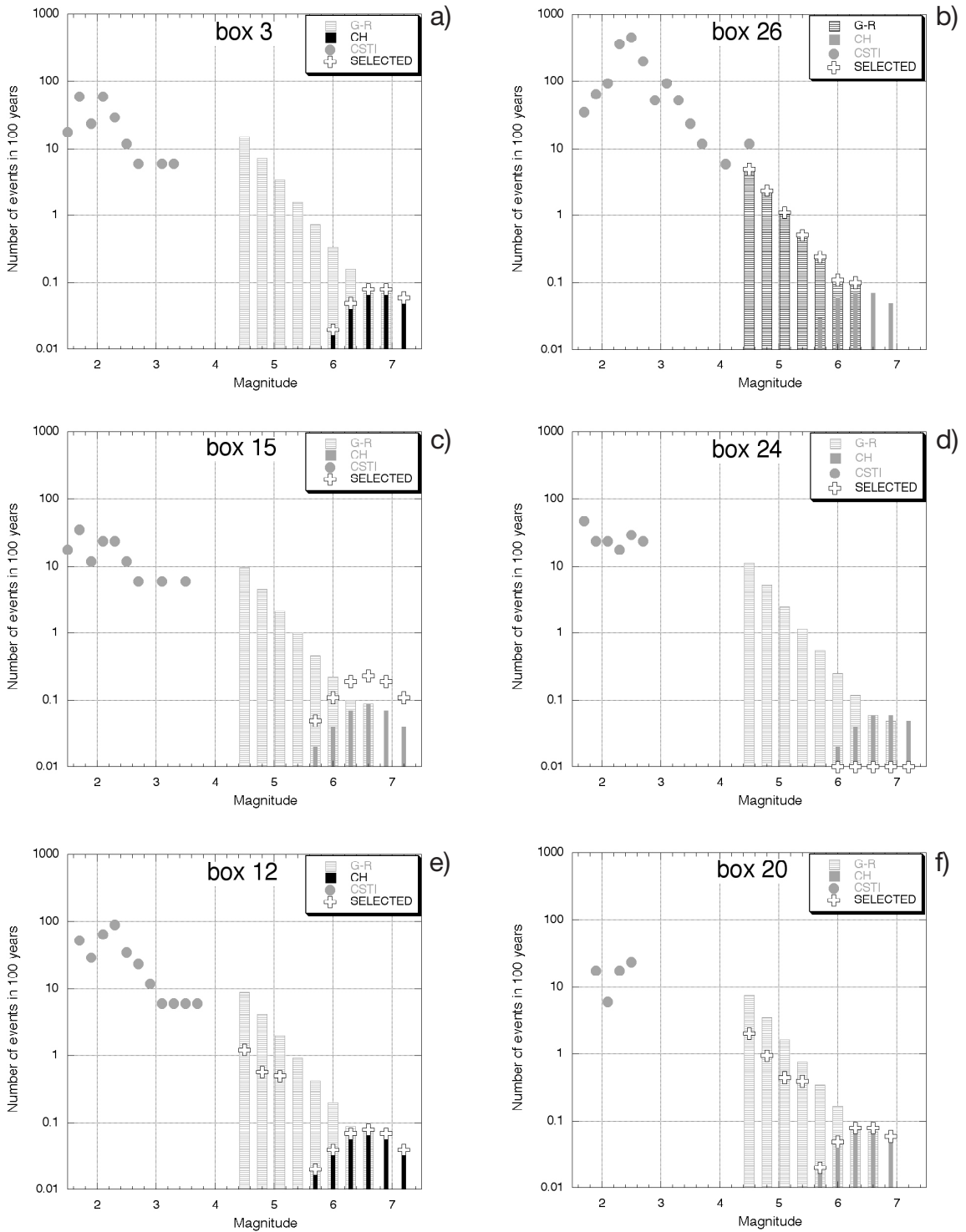


**Fig. 4** - Seismicity rates following different models for some seismogenic boxes. In the legend G-R means Gutenberg-Richter exponential model; CH is a bell-shaped approximation of a characteristic earthquake model; CSTI are experimental rates derived from the events located inside the box in the instrumental catalogue from 1981 to 1996 (CSTI G.d.L., 2001). Crosses mark the rates finally selected for computing Fig. 8: the plusses on the 0.01 axis mean that zero rate are selected for these magnitudes for the source. The black symbol indicates the selected model.

in Fig. 3b) will be taken as reference values in the following. Nevertheless, they alone do not solve the problem of quantifying the whole seismic activity of the boxes/sources, as needed to estimate their impact in seismic hazard assessment. Recurrence models may be divided into two main categories. Some models assume that individual faults generate only a single earthquake magnitude (with some uncertainty) and not small-magnitude events: the “maximum moment” recurrence model (Wesnousky et al., 1983), and the “mean recurrence rate” approach previously described belong to this category. The second group pertains to the models that allow a full range of magnitude to occur on individual faults: the exponential distribution proposed by Gutenberg and Richter (1944) for large regions, but also the “characteristic earthquake” (CH) recurrence model (Schwartz and Coppersmith, 1984), as first defined in Youngs and Coppersmith (1985) belong to this second category. We decided to use, a priori, two well-known earthquake models, tuned on the previously described  $M$  and  $T$  values, and to compare the predicted occurrences with the seismological information available.

Anderson and Luco (1983) first described the use of fault slip rate with an exponential (G-R) recurrence model; here, a G-R distribution with constant b-value taken from a regional study (Peruzza, 1999b) has been anchored and truncated on the  $M_{max}$  and  $T$  values. A Gaussian distribution instead, peaked on  $M_{max}$  and  $T$ , simulates the behaviour of a CH model where small magnitude events are not admitted. Fig. 4 reports the seismicity rates of some sources, comparing those obtained by the previously described geometrical modelling with observa-

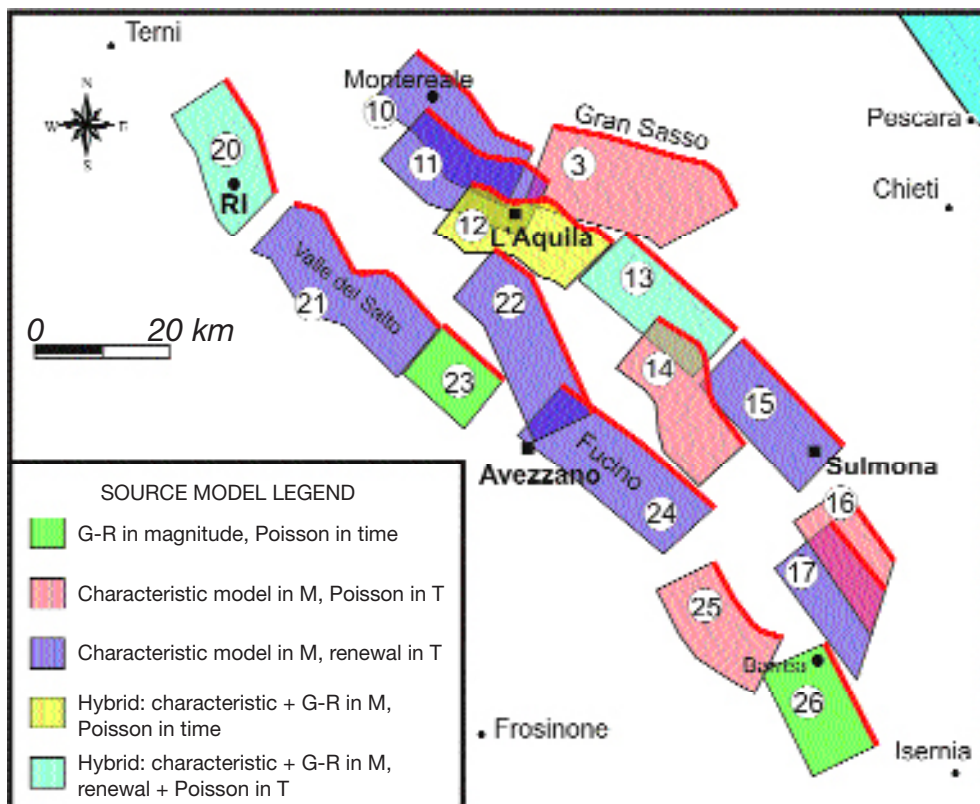


Fig. 5 - Composition of different kinds of source models for the boxes in the Abruzzo region.

tions coming from historical and instrumental earthquake catalogues (CPTI G.d.L., 1999; CSTI G.d.L., 2001). The Gran Sasso and Barrea sources (respectively box 3 and 26) represent the two limit cases where a pure CH model and a pure G-R model seem to be adequate to represent the seismological data. A quite flat distribution of earthquakes with magnitude lower than 3.5, no events during historical times, and paleoseismological evidence of multiple ruptures suggest selecting the CH model for source 3. On the other hand, the G-R behaviour coming from geometrical considerations is very well correlated with the distribution of recent events (CSTI G.d.L., 2001); it is notable that only the tail of the 1984 sequence is located inside the Barrea box, and probably the main shock is affected by mislocation problems of the network of that time (Pace et al., 2002b). Sulmona and Fucino sources (boxes 15 and 24) are examples of CH models where the time dependency may drive to opposite results, as will be described in the following. Other sources (e.g. 12 Aquilano, and 20 Rieti) seem to deviate from simple exponential or Gaussian models. We therefore used hybrid models (as defined by Wu et al., 1995, but in practice very similar to the original definition of the CH recurrence model), where the seismicity rates modelling a CH behaviour for large events ( $M_{max}$ ) have been combined with a G-R exponential model for small-to-moderate events. In these cases the G-R tails are calibrated on magnitudes and occurrence rates of the historical earthquake catalogue.

Fig. 5 summarizes the different models finally adopted for the seismogenic boxes in the Abruzzo region.

### 3. Seismic hazard computation

We now move on to applying the seismogenic source model to the seismic hazard analysis. All the computations have been performed using a traditional code (SEISRISK III, by Bender and Perkins, 1987) in a version modified by LaForge (1996). The results are expressed in peak ground acceleration (PGA) at 90% probability of non-exceedence in 50 years, using the empirical attenuation relationships proposed by Ambraseys et al. (1996).

#### 3.1. Poissonian hazard maps

Poissonian hazard maps are those obtained by the use of distribution models in the assumption of stationarity of the seismicity. They are as follows: the G-R exponential distribution attributed to all the sources (Fig. 6a), the CH model for all the boxes (Fig. 6b), and the rational selection of the most adequate model according to Fig. 5, with the composition in terms of hybrids for some sources (map not shown as very similar to Fig. 6b). Generally speaking, the use of CH models gives higher ground motions at a given probability value: this is explained by the fact that the Gaussian shaped distribution adopted for assigning the seismicity rates introduces contributions even for magnitudes higher than the originally selected  $M_{max}$ . The conservation of the total seismic moment rate is therefore needed, if we want to make the two different models comparable.

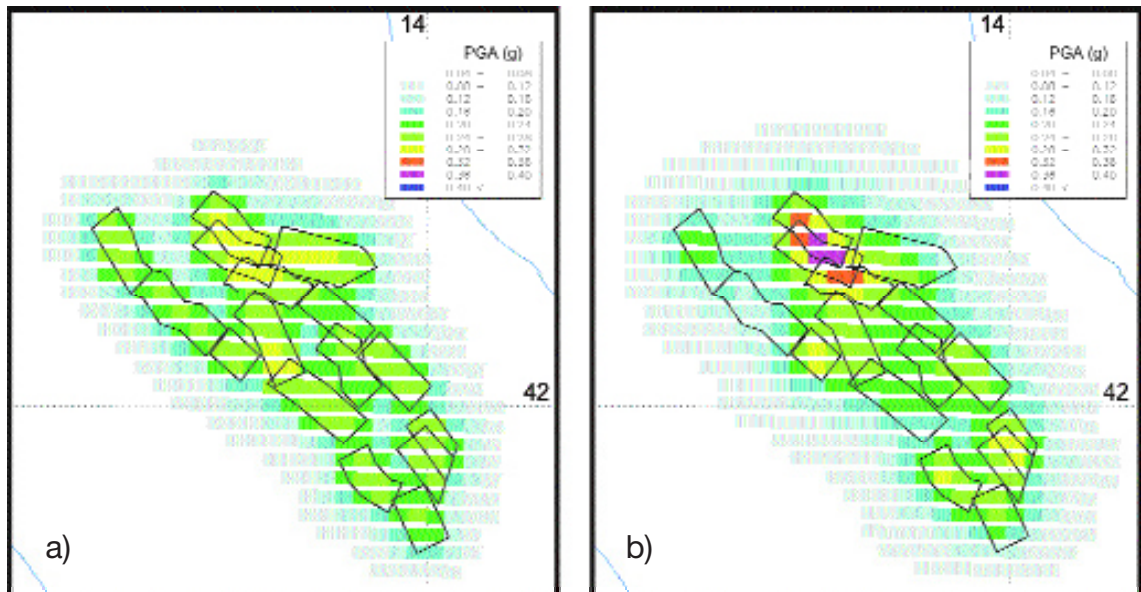


**Fig. 6** - Maps of PGA expected not to be exceeded in 50 years at a 90% probability level: a) using only G-R models; b) using only CH models.

The expected PGA increases from 10 to 30% when the source fault is short, or with overlapping sources (such as boxes 23, 10, 11, 12, 16 and 17). In the first case, the smaller maximum magnitude (or smaller characteristic magnitudes) get shorter recurrences to a given slip rate, producing high hazard; in the second case, closely adjacent faults produce high hazard at sites near both. For longer faults (e.g., boxes 21 and 24), although the recurrence rates are low, they may dominate longer return period ground motions because of the larger maximum magnitudes.

### 3.2. Simplified introduction of time-dependency

Another sensitivity test performed on the source models is related to the introduction of the time-dependence in the seismic hazard analysis. The topic is very debated, and controversial hypotheses are equally well supported (see for example, Stein and Hanks, 1998; Peruzza, 1999c; Cramer et al., 2000), but are out of the aim of this paper. We, therefore, present only the choices adopted to perform a map where the time elapsed since the last event, when known, enters tentatively into the computation. The time between events is modelled by a lognormal distribution with standard deviation 0.4 (see Peruzza et al., 1997 for a full description). The time elapsed since the last event is used to determine the conditional probability of having an event in the next 50 years. Not all the boxes have a dated event associated to them, and therefore, the computation applies only to some sources; Fig. 7 compares the mean recurrence time with the time elapsed since the last major event, and gives the conditional probabilities. Then, using the simplification proposed by Wu et al. (1995), equivalent fictitious seismicity rates have been

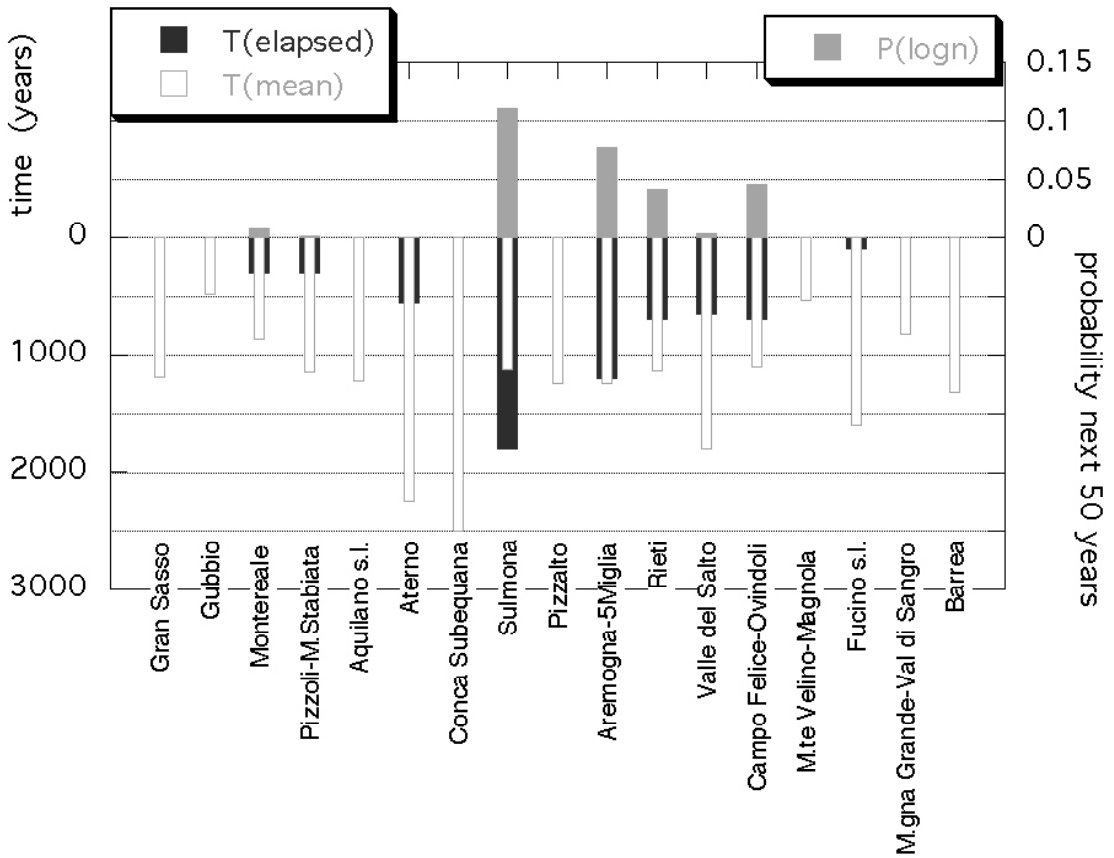


**Fig. 7** - Quantities related to the renewal process adopted for some sources. In the lower part of the graph (axis on the left) mean recurrence time ( $T_6$  in Fig. 3b) and time elapsed since the last event (when available). In the upper part (axis on the right) conditional occurrence probability of an event in the next 50 years (from 2001) using lognormal distribution with variable mean and fixed standard deviation (following Peruzza et al., 1997, see the text).

calculated and introduced in the memory-less code for seismic hazard assessment. The results may be considered approximate computations suitable for engineering applications, and they have been mapped in Fig. 8. The picture is quite different from the one obtained under Poissonian assumptions; the maximum hazard is moved southwards, involving sources that are considered to have been silent for a long time (boxes 15 and 17). On the other hand, sources that have been recently activated (see box 24 Fucino in Fig. 4) disappear from the map. We have to consider, however, that about half of the mapped boxes still remain modelled as time independent, and their hazard may be underestimated, because of the lack of a date for the last event.

### 3.3. Disaggregation analysis in three case sites

Disaggregation analysis has been finally performed in three main localities in the study area, L'Aquila, Avezzano and Sulmona (see location in Fig. 1b). The four seismicity models

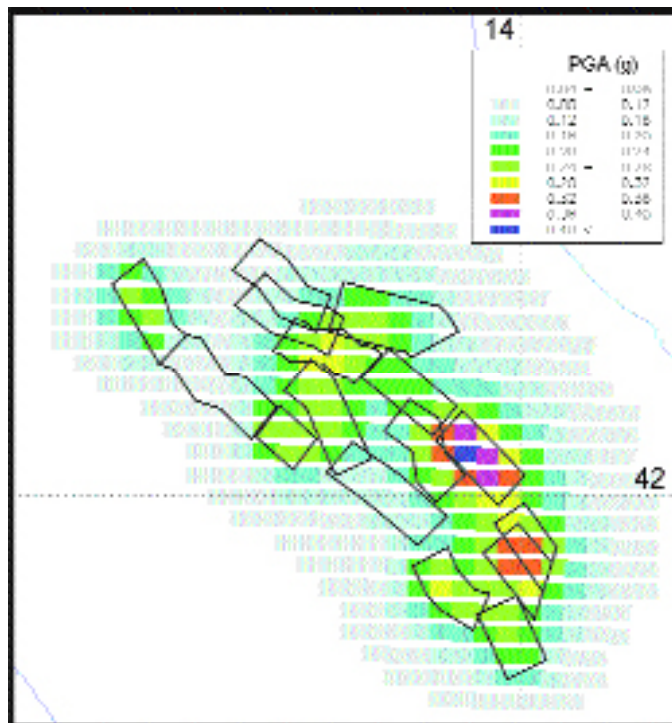


**Fig. 8** - Map of PGA expected not to be exceeded in 50 years at a 90% probability level from 2001, using an hybrid and “time-dependent” models.

previously presented (G-R, CH, composition with hybrids without time-dependency, composition with time-dependency) were processed with a modified version of SEISRISK III (LaForge, 1996) to obtain the contribution of each source to the total hazard. Then, the results for several PGA thresholds at the sites have been plotted in Figs. 9 and 10; columns indicate the different models adopted, rows represent the localities. The analysis refers to mean attenuation values, as in the previous maps, and the PGA thresholds roughly represent significant values of macroseismic intensity, as in the scheme reported for the readers’ simplicity in Table 4. The PGA thresholds are useful to enlighten the behaviour of the probabilistic study at a different level of seismic motion. The disaggregation analysis refers to all the boxes mapped in Fig. 1b, indicated in the x-axis by the source code, regardless from their distance from the study sites.

**Table 4** - Correlation derived from Italian literature between PGA values and macroseismic intensity; D95 stays for Decanini et al. (1995); M92 for Margottini et al. (1992).

PGA (g)	Color (Fig. 9)	I D95	I M92	comments
0.02	Green		III ?	Perception threshold
0.1	Grey		VI	Damage threshold
0.2	Blue	VII	VII-VIII	Significant damage
0.3	Black	~ IX		Heavy damage
0.4	Red	~ X		Many collapses
0.5	Violet	> X		Total collapse

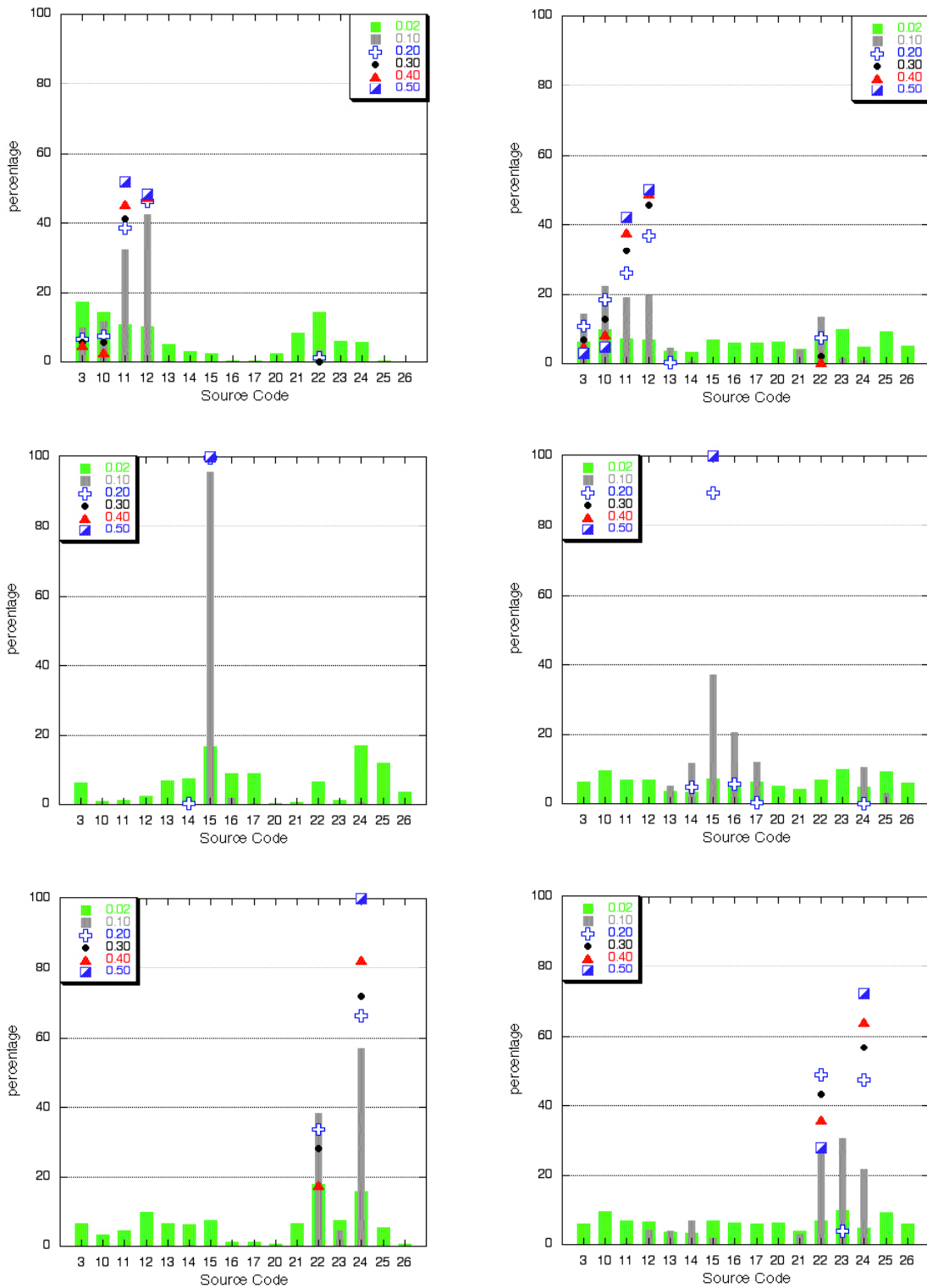


**Fig. 9** - Disaggregation analysis for 2 different seismicity models (left column G-R; right column CH) at three main localities (first row L'Aquila, second row Sulmona and third row Avezzano, see Fig. 1b for their location). Colours and symbols reported in the legends indicate PGA thresholds (see also Tab. 4).



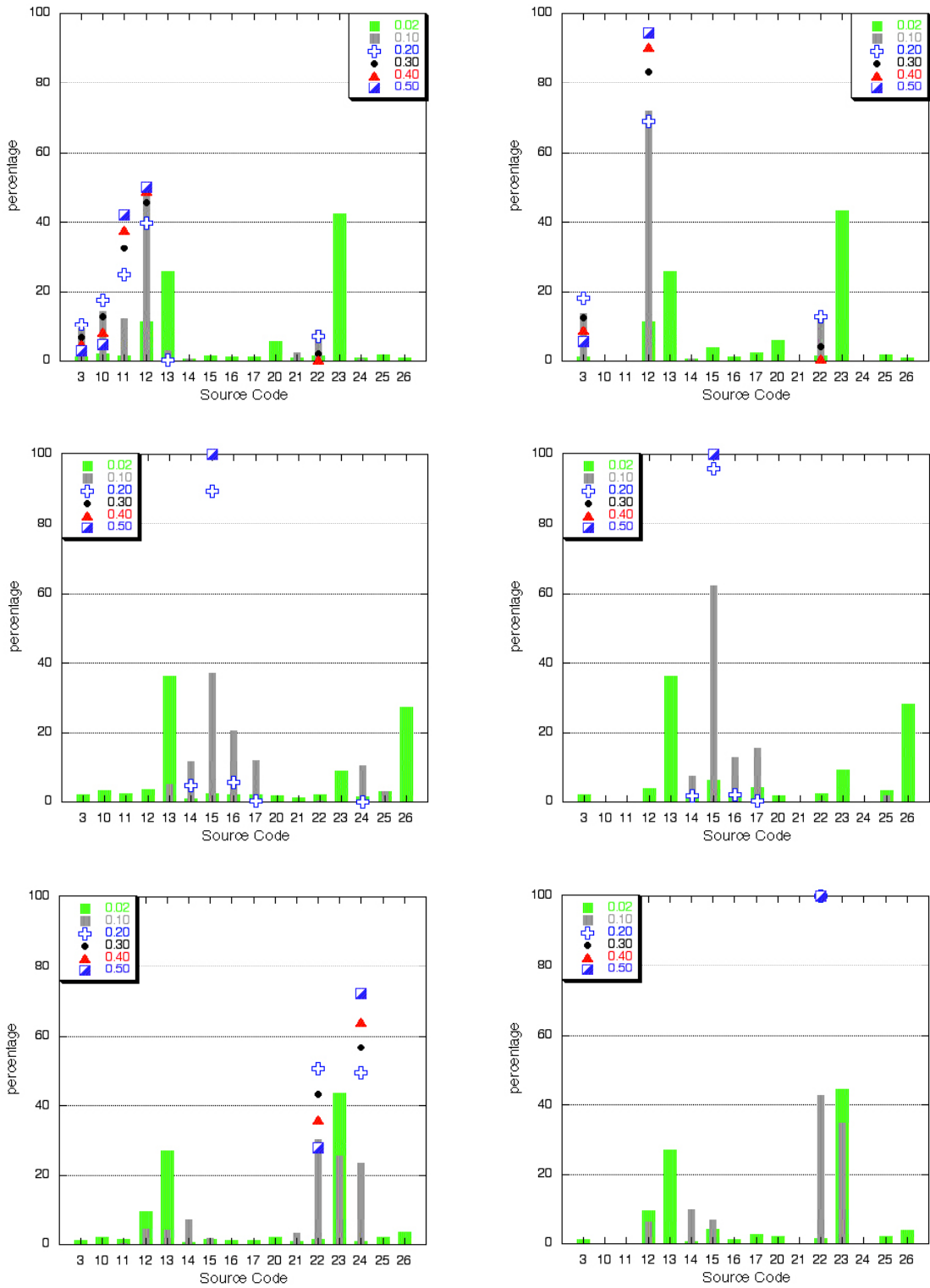


**Fig. 10** - Disaggregation analysis for 2 different seismicity models (left column time-independent hybrid; right column time-dependent hybrid) at three main localities (first row L’Aquila, second row Sulmona and third row Avezzano, see Fig. 1b for their location). Colours and symbols reported in the legends indicate PGA thresholds (see also Tab. 4).

In the hypothesis of a pure G-R behaviour of magnitude distribution (left column of Fig. 9), the hazard is dominated by the box where the site is located, at least as far as damaging levels of ground motion are concerned. It is interesting to note the exclusive contribution of box 15 at Sulmona, the double influence of boxes 22 and 24 at Avezzano, and the more complex interaction of four sources (11, 12 and, subordinately, 3 and 10) at L'Aquila. The coexistence of all these active structures is still an open question, on a geological basis, but, if accepted, it significantly raises the probability of occurrence of heavy damage at L'Aquila. The situation is very different at perceptible levels of ground motion (PGA value 0.02). Earthquakes felt in the test sites may belong to all the sources that lie in an about 20 km radius from the investigated localities; this influence distance obviously increases when intrinsic uncertainties in attenuation, or local amplification factors, are taken into account.

The CH model for all the sources (right column in Fig. 9) increases, in general, the contribution of different boxes in building up the hazard of the intermediate classes of ground motion. The first damage threshold, indicated by the grey bar, is now caused by many sources, usually more than seven, that are in the neighbourhood of the sites. This can be the effect of a lower probability of occurrence for quakes with magnitude different from the characteristic one (remember that the contribution of sources is given as a percentage, not as absolute value), but also a bias induced by the bell-shaped seismicity rates, that introducing some magnitude classes higher than  $M_{max}$  increases the global seismicity. As a paradox, these results suggest great care before abandoning Poissonian hypotheses for occurrences at the site, in favour of more complex time-dependent models, when the investigated localities are surrounded by many CH sources.

The left column in Fig. 10 is the rational composition of G-R and CH magnitude models, in accordance with seismological knowledge; the conventional exponential-time model is used. The disaggregation results of CH and hybrid models are very similar for damaging levels; the contribution of some boxes becomes notable for small shakings, when they have been considered hybrid sources, and it is due to the G-R tails for the small events.

The right column of Fig. 10 incorporates also renewal processes by means of equivalent seismicity, as previously described. The magnitude models are the same as the previous column, but some boxes have been turned off by the very low probability of occurrences of a major event reported in Fig. 7. Four boxes (15, 17, 20 and 22) enhanced their contribution because of the time elapsed from the last event.

L'Aquila appears now to be critically controlled by the activity of box 12 Aquilano, a poorly known source that requires further investigations, especially concerning associated earthquakes; the Gran Sasso (3) and the Campo Felice – Ovindoli (22) sources are also important, as they are capable of causing potential damage to the city.

Sulmona continues to be threatened dominantly by box 15, even if the nearby boxes 14, 16 and 17 can reach the level of heavy damage too. It has to be mentioned also that the seismic potential of the area towards the Adriatic Sea is underestimated, as no individual sources based on geological evidence have, till now, been proposed to accommodate the significant earthquakes reported in the catalogue.

Finally, the high shaking hazard in Avezzano is now dominated by source 22 (Campo Felice - Ovindoli), because the Fucino one (24) has been diminished by the recent occurrence of the

1915 event. About the same percentage (40%) of the damaging level hazard was contributed by the westernmost Monte Velino-Magnola source, which is also the source mainly responsible for potential felt earthquakes, together with the north-easternmost Aterno source (13).

The comparison of this disaggregation study with the felt shaking histories at the site (Monachesi and Stucchi, 1996) may be very useful as a check on the reliability of the proposed model, and therefore on the forecast of future occurrences. We started to compare the capability of generating shaking of different levels from the Poissonian hybrid model (left column in Fig. 10) with the felt data in the study sites. As an example, the heavy damage reported in Avezzano and in L'Aquila in relation to the 1349 earthquake are in agreement with the predicted high shakings associated with 22 box. On the other hand, they are difficult to explain (without invoking directivity anomalies and/or site effects) if linked to source 21 (Valle del Salto), the adjacent source to which historical data may be equally well associated. The felt history of Sulmona confirms the highest level of seismic hazard suggested by Fig. 8. The stronger shaking of the 1915 Fucino earthquake is compatible with the prediction of box 24, whilst the 1905 Sulmona event, with its low energy, contrasts with the hypothesis of a CH model for source 15. Big events like the 1349 and 1456 ones are again difficult to be accommodated by the hybrid model proposed, and similarly the shakings expected from boxes 14, 16 and 17 apparently do not have any correspondent shakings in the Sulmona time history. What is much more evident, anyway, is the lack of reliable, geologically-constrained sources for the easternmost and southernmost earthquakes, that expressed their damage capability in history with the 1706 (Maiella) and 1933 (Lama dei Peligni) earthquakes.

Future efforts in this kind of analysis may increase the quality and constraints of earthquake-source association, and drive research towards key structure-events.

#### 4. Conclusions

The sensitivity analyses presented try to suggest criteria and constraints to define seismogenic sources useful in seismic hazard analysis. The geological and structural knowledge of the study region is the first key element for interpreting the known seismicity, and for extrapolating the non-observed one.

Realistic simulations of the site seismic histories have to be based on a careful selection of a wide range of hypotheses about seismicity models, where many approximations are needed. The evaluation of the uncertainties introduced by these approximations is the main topic that calls for further efforts in the future.

**Acknowledgments.** The present study has been performed in the frame and with the financial support of the GNDT Project "Probable earthquakes in Italy from year 2000 to 2030: guidelines for determining priorities in seismic risk mitigation" (coordinated by A. Amato), research contractor OGS. The GeoSisLab Group of the Chieti University (G. Lavecchia coord.) elaborated the seismogenic model for central Italy, partially used in this paper. Special thanks go to D.M. Perkins and K.J. Coppersmith, for their thoughtful and constructive review of the manuscript.

## References

- Amato A., Azzara R., Chiarabba C., Cimini G.B., Cocco M., Di Bona M., Margheriti L., Mazza S., Mele F., Selvaggi G., Basili A., Boschi E., Courboux F., Deschamps A., Gaffet S., Bittarelli G., Chiaraluca L., Piccinini D. and Ripepe M.; 1998: *The 1997 Umbria-Marche, Italy, earthquake sequence; a first look at the main shocks and aftershocks*. Geophysical Research Letters, **25**, 2861-2864.
- Ambraseys N.N., Simpson K.A. and Bommer J.J.; 1996: *Prediction of horizontal response spectra in Europe*. Earthquake Engineering and Structural Dynamics, **25**, 371-400.
- Anderson J.G. and Luco J.E.; 1983: *Consequences of slip rate constraints on earthquake recurrence relations*. Bull. Seismol. Soc. Am., **73**, 471-496.
- Barba S. and Basili R.; 2000: *Analysis of seismological and geological observations for moderate-size earthquakes; the Colfiorito fault system (central Apennines, Italy)*. Geophysical Journal International, **141**, 241-252.
- Barchi M., Lavecchia G., Galadini F., Messina P., Michetti A.M., Peruzza L., Pizzi A., Tondi E. and Vittori E. (eds); 2000: *Sintesi delle conoscenze sulle faglie attive in Italia Centrale: parametrizzazione ai fini della caratterizzazione della pericolosità sismica*. CNR-GNDT, Volume congiunto dei Progetti 5.1.2, 6a2, 5.1.1, Roma, 62 pp.
- Bender B. and Perkins D.M.; 1987: *SEISRISK III; a computer program for seismic hazard estimation*. U. S. Geological Survey, Reston, VA, United States, Open File Report.
- Blumetti A.M.; 1995: *Neotectonic investigation and evidence of paleoseismicity in the epicentral area of the January-February 1703, central Italy, earthquakes*. In: Serva L. and Slemmons D.B. (eds), *Perspectives in paleoseismology*, A.E.G. Special Publication n. 6, pp. 83-99.
- Boncio P., Brozzetti F. and Lavecchia G.; 2000: *Architecture and seismotectonics of a regional low-angle normal fault zone in central Italy*. Tectonics, **19**, 1038-1055.
- Boncio P., Lavecchia G. and Pace B.; 2002: *A new seismogenic sources model in Central Italy, based on structural-geological data*. Tectonophysics, submitted.
- Bonilla M.G., Mark R.K. and Lienkaemper J.J.; 1984: *Statistical relations among earthquake magnitude, surface rupture length, and surface fault displacement*. Bull. Seismol. Soc. Am., **74**, 2379-2411.
- CPTI G.d.L., Boschi E., Gasperini P., Valensise G., Camassi R., Castelli V., Stucchi M., Rebez A., Monachesi G., Barbano M.S., Albini P., Guidoboni E., Ferrari G., Mariotti D., Comastri A. and Molin D.; 1999: *Catálogo Parametrico dei Terremoti Italiani*. ING, GNDT, SGA, Bologna, 92 pp.
- Cramer C.H., Petersen M.D., Cao T., Topozada T.R. and Reichle M.; 2000: *A time-dependent probabilistic seismic-hazard model for California*. Bull. Seismol. Soc. Am., **90**, 1-21.
- CSTI G.d.L.; 2001: *Catálogo strumentale dei terremoti "italiani" dal 1981 al 1996, versione 1.0*. A cura di: P. Augliera, M. Cattaneo, H. Coppari, R. DiGiovannibattista, G. Durì, M. Fraccipini, P. Gasperini, A. Gervasi, A. Govoni, I. Guerra, A. Marchetti, P. Marsan, G. Milana, G. Monachesi, A. Moretti, L. Moroncelli, L. Orlanducci, S. Parolai, G. Renner, D. Spallarossa, L. Trojani and G. Vannucci, ING-GNDT, Bologna, CD-Rom.
- D'Addezio G., Masana E. and Pantosti D.; 2001: *The Holocene paleoseismicity of the Aremogna-Cinque Miglia Fault (Central Italy)*. Journal of Seismology, **5**, 181-205.
- Decanini L., Gavarini C. and Mollaioli F.; 1995: *Proposta di definizione delle relazioni tra intensità macrosismica e parametri del moto del suolo*. In: 7° Convegno Nazionale "L'ingegneria sismica in Italia" 25-28/9/1995, Siena, pp. 63-72.
- Field E.H., Johnson D.D. and Dolan J.F.; 1999: *A mutually consistent seismic-hazard source model for Southern California*. Bull. Seismol. Soc. Am., **89**, 559-578.
- Galadini F. and Galli P.; 2000: *Active tectonics in the Central Apennines (Italy); input data for seismic hazard assessment*. Natural Hazards, **22**, 225-270.
- Galadini F. and Galli P.; 2001: *Archaeoseismology in Italy; case studies and implications on long-term seismicity*. Journal of Earthquake Engineering, **5**, 35-68.

- Gutenberg B. and Richter C.F.; 1944: *Frequency of earthquakes in California*. Bull. Seismol. Soc. Am., **34**, 185-188.
- Hanks T.C. and Kanamori H.; 1979: *A moment magnitude scale*. J. Geoph. Res., **84**, 2348-2350.
- Hodgkinson K.M., Stein R.S. and King G.C.P.; 1996: *The 1954 Rainbow Mountain-Fairview Peak-Dixie Valley earthquakes; a triggered normal faulting sequence*. J. Geoph. Res., **101**, 25,459-25,471.
- LaForge R.; 1996: *Implementation of SEISRISK III*. USGS, Colorado, Boulder, Open File.
- Lavecchia G., Boncio P., Brozzetti F., Stucchi M. and Leschiutta I.; 2002: *New criteria for seismotectonic zoning in Central Italy; insights from the Umbria-Marche Apennines*. Boll. Soc. Geol. It., Vol. Spec. **1**(2002), 881-891.
- Mai P.M. and Beroza G.C.; 2000: *Source scaling properties from finite-fault-rupture models*. Bull. Seismol. Soc. Am., **90**, 604-615.
- Margottini C., Molin D. and Serva L.; 1992: *Intensity versus ground motion; A new approach using Italian data*. Engineering Geology, **33**, 45-58.
- Michetti A.M., Brunamonte F., Serva L. and Vittori E.; 1996: *Trench investigations of the 1915 Fucino earthquake fault scarps (Abruzzo, central Italy); geological evidence of large historical events*. J. Geoph. Res., **101**, 5921-5936.
- Monachesi G. and Stucchi M.; 1996: *DOM 4.1; un database di osservazioni macrosismiche di terremoti di area italiana al di sopra della soglia del danno*. GNDT, Milano, <http://emidius.mi.ingv.it/DOM/>, Open file report.
- Pace B.; 2001: *Sorgenti sismogenetiche in Appennino Centrale; definizione ed applicazione alle stime di pericolosità sismica*. Ph.D Thesis, Dipartimento di Scienze della Terra, Università di Camerino, Camerino, 144 pp.
- Pace B., Peruzza L., Lavecchia G. and Boncio P.; 2002a: *Seismogenic sources in Central Italy; from causes to effects*. Mem. Soc. Geol. It., in press.
- Pace B., Boncio P. and Lavecchia G.; 2002b: *The 1984 Abruzzo earthquake (Italy); an example of seismogenic process controlled by interaction between differently-oriented synkinematic faults*. Tectonophysics, **350**, 237-254.
- Pantosti D., D'Addezio G. and Cinti F.R.; 1996: *Paleoseismicity of the Ovindoli-Pezza fault, central Apennines, Italy; A history including a large, previously unrecorded earthquake in the Middle ages (860-1300 AD)*. J. Geoph. Res., **101**, 5937-5959.
- Pantosti D. and Valensise G.; 1990: *Faulting mechanism and complexity of the November 23, 1980, Campania-Lucania earthquake, inferred from surface observations*. J. Geoph. Res., **95**, 15,319-15,341.
- Peruzza L. (ed); 1999a: *Progetto MISHA. Metodi Innovativi per la Stima dell'HAzard - Applicazione all'Italia Centrale*. GNDT, Studio Gamma, Trieste, 176 pp.
- Peruzza L.; 1999b: *Analisi di sensibilità all'introduzione di sorgenti lineari e trattamento time-dependent*. In: Peruzza L. (ed), Progetto MISHA. Metodi Innovativi per la Stima dell'HAzard - Applicazione all'Italia Centrale, GNDT, Roma, pp. 139-162.
- Peruzza L.; 1999c: *Modello di segmentazione per l'Italia Centrale; dal consenso sulle strutture, alla probabilità di accadimento di un terremoto maggiore*. In: Peruzza L. (ed), Progetto MISHA. Metodi Innovativi per la Stima dell'HAzard - Applicazione all'Italia Centrale, GNDT, Roma, pp. 47-57.
- Peruzza L., Pantosti D., Slejko D. and Valensise L.; 1997: *Testing a New Hybrid Approach to Seismic Hazard Assessment; an Application to the Calabrian Arc (Southern Italy)*. Natural Hazards, **14**, 113-126.
- Scholz C.H.; 1990: *The mechanics of earthquakes and faulting*. Cambridge University Press, Cambridge, 439 pp.
- Schwartz D.P. and Coppersmith K.J.; 1984: *Fault behaviour and characteristic earthquakes; examples from the Wasatch and San Andreas fault zones*. In: Fault behaviour and the earthquake generation process, American Geophysical Union, Washington, DC, pp. 5681-5698.
- Selvaggi G.; 1998: *Spatial distribution of horizontal seismic strain in the Apennines from historical earthquakes*. Annali di Geofisica, **41**, 241-251.
- Stein R.S. and Barrientos S.E.; 1985: *Planar high-angle faulting in the Basin and Range; geodetic analysis of the 1983 Borah Peak, Idaho, earthquake*. J. Geoph. Res., **90**, 11,355-11,366.

- Stein R.S. and Hanks T.C.; 1998: *M* > or = 6 earthquakes in southern California during the twentieth century; no evidence for a seismicity or moment deficit. Bull. Seismol. Soc. Am., **88**, 635-652.
- Tondi E.; 2000: *Geological analysis and seismic hazard in the central Apennines (Italy)*. Journal of Geodynamics, **29**, 517-534.
- Vakov A.V.; 1996: *Relationships between earthquake magnitude, source geometry and slip mechanism*. Tectonophysics, **261**, 97-113.
- Valensise G. and Pantosti D.; 2001a: *The investigation of potential earthquake sources in peninsular Italy; a review*. Journal of Seismology, **5**, 287-306.
- Valensise G. and Pantosti D.; 2001b: *Database of Potential Sources for Earthquakes larger than M 5.5 in Italy*. Annali di Geofisica, **44**(4), 1-964.
- Wells D.L. and Coppersmith K.J.; 1994: *New empirical relationships among magnitude, rupture length, rupture width, rupture area, and surface displacement*. Bulletin of the Seismological Society of America, **84**, 974-1002.
- Wesnousky S., Scholz C.H., Shimazaki K. and Matsuda T.; 1983: *Earthquake frequency distribution and mechanics of fault*. J. Geoph. Res., **88**, 9331-9340.
- Wu S.C., Cornell C.A. and Winterstein S.R.; 1995: *A hybrid recurrence model and its implication on seismic hazard results*. Bull. Seismol. Soc. Am., **85**, 1-16.
- Youngs R.R. and Coppersmith K.J.; 1985: *Implication of fault slip rates and earthquake recurrence models to probabilistic seismic hazard estimates*. Bull. Seismol. Soc. Am., **75**, 939-964.